Scientific Research Publishing

Computational Molecular Bioscience, 2026, 16(3), 52-72
https://www.scirp.org/journal/cmb
ISSN Online: 2165-3453
ISSN Print: 2165-3445

Influence of the Nature of the Azo Ligand on the Structural, Electronic, and Spectroscopic Properties of Ruthenium $RuCl_2L_2$ Complexes: A Comparative DFT and TD-DFT Study

N'Guessan Kouakou Nobel[1], Kangah Niamké Jean Baptiste[1], Koné Mamadou Guy-Richard[1], Koudjina Simplice[2], Ouattara Wawohinlin Patrice[1], Ouattara Lamoussa[3], Dembele Georges Stéphane[1], Bamba Kafoumba[1], Ziao Nahossé[1]

[1]Laboratory of Thermodynamics and Environmental Physical Chemistry, UFR SFA, Nangui Abrogoua University, Abidjan, Côte d'Ivoire
[2]Laboratory of Chemical Physics-Materials and Molecular Modeling (LCP3M), University of Abomey-Calavi (UAC), Cotonou, Bénin
[3]Faculty of Marine Sciences, SAN PEDRO Polytechnic University, San Pedro, Côte d'Ivoire
Email: nkouakounobel777@gmail.com

How to cite this paper: Nobel, N.K., Baptiste, K.N.J., Guy-Richard, K.M., Simplice, K., Patrice, O.W., Lamoussa, O., Stéphane, D.G., Kafoumba, B. and Nahossé, Z. (2026) Influence of the Nature of the Azo Ligand on the Structural, Electronic, and Spectroscopic Properties of Ruthenium $RuCl_2L_2$ Complexes: A Comparative DFT and TD-DFT Study. *Computational Molecular Bioscience*, **16**, 52-72.
https://doi.org/10.4236/cmb.2026.163004

Received: May 10, 2026
Accepted: September 21, 2026
Published: September 24, 2026

Abstract

This study examines the influence of the number of nitrogen atoms in azo ligands on the geometric, thermodynamic, electronic, and spectroscopic properties of the trans isomers (γ and δ) of ruthenium (II) complexes of the formula $RuCl_2L_2$ (L = azben, azpy, or papm). The calculations were performed using density functional theory (DFT) and time-dependent density functional theory (TD-DFT) at the B3LYP/Lanl2DZ level to determine the optimized structures, thermodynamic parameters, reactivity descriptors, electronic interactions, and electronic absorption properties. The results show that substituting pyridine with pyrimidine has little effect on the geometry of the complexes. However, the substitution of pyridine with phenyl, in the case of the γ-$RuCl_2(azben)_2$ isomer, profoundly alters the complex's octahedral structure. Also, it significantly alters their stability and reactivity. At 298.15 K, the formation of the $RuCl_2(papm)_2$ and $RuCl_2(azpy)_2$ isomers is spontaneous and exothermic, whereas the formation of the $RuCl_2(azben)_2$ isomers is thermodynamically unfavorable under the same conditions. The $RuCl_2(azpy)_2$ complexes appear to be the most thermodynamically stable. Analysis of frontier orbitals and global reactivity descriptors indicates that replacing azopyridine with azobenzene increases the complexes' electronic reactivity. In particular, the γ-$RuCl_2(azben)_2$ isomer exhibits the greatest affinity for interactions with

DNA bases, making it a promising candidate for anticancer applications. Furthermore, TD-DFT calculations reveal that all complexes absorb in the visible spectrum via MLCT (Metal-to-Ligand Charge Transfer) transitions. These optical properties suggest that these compounds could serve as promising photosensitizers for dynamic cancer phototherapy.

Keywords

Ruthenium Complexes, Azo Ligands, DFT, TD-DFT, Electronic Reactivity, MLCT, Dynamic Phototherapy, Cancer

1. Introduction

Compounds containing the azo group (-N=N-) constitute an important family of chromophores with numerous applications in the food, cosmetics, dyes, textile, solar energy, and pharmaceutical industries [1] [2]. The interest in this chemical function stems from the physicochemical properties and biological activities that result from its combination with various aromatic or heteroaromatic rings, such as benzene, pyridine, or pyrimidine. Thus, azo derivatives represent a promising class of bioactive compounds with antifungal, anti-inflammatory, antitubercular, and anticancer properties [3].

Among these heterocycles, pyridine and pyrimidine play an important role in medicinal chemistry due to their strong ability to modulate the electronic and biological properties of the molecules that contain them. The bonding of the azo group (-N_1=N_2-) to benzene via the N_1 atom and, respectively, to benzene, pyridine, or pyrimidine via the N_2 atom results in the ligands azobenzene (azben), 2-phenylazopyridine (azpy) [4], and 2-phenylazopyrimidine (papm) [5]. The corresponding molecular structures are shown in **Figure 1**.

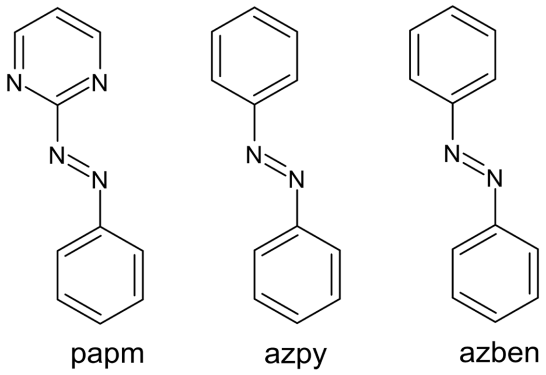

Figure 1. 2D structure of the azo ligands studied.

These three ligands differ primarily in the number of nitrogen atoms present in the aromatic ring bonded to the N_2 atom of the azo group. This structural difference is likely to significantly influence the electronic distribution, the coordina-

tion capacity, and, consequently, the physicochemical and biological properties of the compounds. Indeed, nitrogen atoms possess non-bonding electron pairs that can alter the ligand's electron density, its affinity for metal centers, as well as its solubility, bioavailability, metabolism, and interaction with biological targets [6]. Many therapeutic molecules, in fact, exploit this structural feature. Azo ligands also constitute an important family of bidentate ligands capable of stabilizing ruthenium ions at oxidation states +II and +III [7]. Azo ligands are also an important class of bidentate ligands capable of stabilizing ruthenium ions in oxidation states +II and +III [7]. All $RuCl_2L_2$ complexes were treated as neutral Ru(II) species containing two anionic chloride ligands and two neutral azo ligands. The calculations were carried out using a singlet ground state (multiplicity = 1). The total charge and multiplicity of each molecular system were explicitly specified in the computational input files. If applicable: Alternative spin states were also examined and found to be higher in energy than the singlet state. The resulting $RuCl_2L_2$ complexes (L = azo ligand) exhibit particularly interesting electronic, photochemical, and biological properties, which are exploited in both dye-sensitized solar cells and the development of new anticancer agents [7]-[9]. In particular, several experimental and theoretical studies have shown that ruthenium complexes derived from 2-phenylazopyridine used as reference systems in this work exhibit promising activity against various types of cancer, notably colon, breast, and throat cancers [10] [11].

The complexation of ruthenium derived from the $RuCl_3{\cdot}3H_2O$ precursor by azopyridine ligands leads to the formation of five geometric isomers designated α-Cl, β-Cl, γ-Cl, δ-Cl, and ε-Cl [12] [13]. The α-Cl, β-Cl, and ε-Cl isomers belong to the *cis* configuration, while the γ-Cl and δ-Cl isomers exhibit a *trans* configuration, defined by the relative arrangement of the two chloride ligands around the metal center. Previous studies have shown that *trans* isomers generally possess greater stability and more promising biological properties. For this reason, only the γ-Cl and δ-Cl isomers will be considered in this study.

The main objective of this work is to evaluate, using density functional theory (DFT), the effect of replacing the pyridine ring in azopyridine with a benzene or pyrimidine ring on the geometric, electronic, and spectroscopic properties of the γ-$RuCl_2(azpy)_2$ and δ-$RuCl_2(azpy)_2$ complexes. More specifically, this study aims to highlight the influence of the number of nitrogen atoms present in the aromatic ring of the azo ligand on the stability, reactivity, and optical properties of the ruthenium complexes.

To achieve this objective, density functional theory (DFT) is used as the computational method. Recognized for its excellent balance between accuracy and computational cost, this approach is now one of the most powerful tools for modeling molecular and organometallic systems [14]. Based on solving the Schrödinger equation using the electron density, DFT allows for the determination, with good accuracy of the optimized structures, electronic properties, reactivity descriptors, and spectroscopic properties of the compounds under study.

2. Materials and Methods

2.1. Geometric Optimization and Frequency Analysis

The molecular systems studied in this work are obtained by substituting the pyridine ring of the γ-Cl and δ-Cl isomers of the reference complex $RuCl_2(azpy)_2$ with a benzene or pyrimidine ring. This strategy led to a comparative study of six ruthenium complexes, with the aim of evaluating the influence of the number of nitrogen atoms present in the ligand's aromatic ring on their structural, electronic, and spectroscopic properties.

Quantum chemistry calculations are performed within the framework of density functional theory (DFT), using the Becke three-parameter hybrid functional combined with the Lee-Yang-Parr correlation functional (B3LYP) [15]. This choice is motivated by the fact that B3LYP offers an excellent balance between accuracy and computational cost. This functional has been extensively validated for the study of transition metal complexes, particularly those of ruthenium, and satisfactorily reproduces the geometric parameters, electronic properties, and relative energies of the various isomers.

Geometric optimizations and vibrational frequency calculations are performed using the B3LYP/LanL2DZ theory [16]. The choice of the LanL2DZ basis set is justified by the presence of the ruthenium atom, a transition metal for which this basis set incorporates an Effective Core Potential (ECP). This approach allows for the relativistic effects of inner-shell electrons to be taken into account while significantly reducing computational cost, without compromising the quality of the results.

All calculations were performed using the Gaussian software [17]. Following geometric optimization, a frequency calculation was systematically performed to verify the nature of the obtained structures. The absence of imaginary frequencies confirms that each optimized structure corresponds to a local minimum on the potential energy surface, *i.e.*, a stable ground state.

The optimized structures then serve as the basis for determining the main geometric parameters (bond lengths and angles around the metal center), thermodynamic quantities (enthalpy, entropy, and Gibbs free energy), as well as electronic properties such as the energies of the boundary orbitals (HOMO and LUMO). These parameters enable the analysis of the complexes' stability, their chemical reactivity, and their potential ability to interact with biological systems or exhibit photochemical properties.

2.2. Thermodynamic Quantities of Reactions

The complexes under study are assumed to be obtained experimentally by the reaction between ruthenium trichloride trihydrate, $RuCl_3{\cdot}3H_2O$, and two azo ligands L (L = azpy, azben, or papm), according to the following overall reaction:

$$RuCl_3{\cdot}3H_2O + 2L \rightarrow RuCl_2L_2 + \frac{1}{2}Cl_2 + 3H_2O$$

The thermodynamic parameters associated with the formation reactions were calculated from the electronic energies obtained at the optimized geometries, including zero-point energy and thermal corrections derived from frequency calculations at 298.15 K. The Gibbs free energies were subsequently obtained by combining the corresponding enthalpic and entropic contributions.

All thermodynamic quantities were calculated for the gas phase at 298.15 K and under the standard-state convention adopted in the calculations. To evaluate the thermodynamic feasibility of this reaction, the standard thermodynamic properties of the reactants and products are determined based on calculations performed using the Gaussian software. The values for the standard enthalpy of formation ($\Delta_f H^\circ$), the standard Gibbs free energy of formation ($\Delta_f G^\circ$), and the standard entropy of formation ($\Delta_f S^\circ$) are extracted from the calculation output files.

These data are then used to calculate the changes in reaction enthalpy ($\Delta_r H^\circ$), Gibbs free energy of reaction ($\Delta_r G^\circ$), and reaction entropy ($\Delta_r S^\circ$), in accordance with Hess's law. These parameters allow us to assess whether the reaction is endothermic or exothermic, its spontaneity at the given temperature, and the evolution of disorder during the formation of the ruthenium complexes under study.

2.3. Global Reactivity Descriptors

Boundary orbitals play a crucial role in interpreting the chemical reactivity of molecular systems [18]. In particular, the energies of the highest occupied molecular orbital (HOMO) and the lowest unoccupied molecular orbital (LUMO) provide essential information on a molecule's ability to donate or accept electrons [19]. These parameters thus provide a relevant basis for evaluating the stability and reactivity of the complexes under study.

In this work, several global reactivity descriptors, derived from the hard and soft acid-base (HSAB) theory developed by Pearson [20], are calculated and analyzed. These include the energy gap between the HOMO and LUMO orbitals (energy gap, ΔE), the chemical potential (μ), the chemical hardness (η), and the electrophilicity index (ω) [21]. These descriptors are used to characterize the electronic stability of the complexes, their ability to transfer charge, and their behavior with respect to nucleophilic or electrophilic species.

The values of these various descriptors are determined from the energies of the boundary orbitals according to the following relationships:

$$\Delta E = E_{LUMO} - E_{HOMO}\ ;\quad \mu = -\frac{PI + AE}{2}\ ;\quad \eta = (PI - AE)\ ;\quad \omega = \frac{\mu^2}{2\eta}$$

where $AE = -E_{LUMO}$ is the electron affinity, which characterizes a molecule's susceptibility to nucleophilic attack, and $PI = -E_{HOMO}$ is the ionization potential, which characterizes a molecule's susceptibility to electrophilic attack.

2.4. Analysis of the Natural NBO Population

The Natural Bond Orbital (NBO) method is a widely used post-processing analysis tool for interpreting the results of quantum chemistry calculations [22]. It de-

scribes the electronic structure of molecules using localized orbitals, which are similar to the classical representation of chemical bonds and non-bonding doublets.

This method highlights donor-acceptor interactions between occupied and unoccupied orbitals, which are responsible for phenomena such as electronic delocalization, hyperconjugation, and charge transfer. NBO analysis also provides the natural populations, atomic charges, and stabilization energies associated with these interactions, thereby offering a detailed description of the nature of chemical bonds.

In this work, NBO analysis is used to characterize the electronic interactions within the studied ruthenium complexes, to evaluate the strength of metal-ligand bonds, and to highlight the effect of azo ligand substitution on the electronic distribution and stability of the complexes. It thus complements the geometric, energetic, and orbital analyses obtained by density functional theory (DFT), providing a more refined chemical interpretation of the results.

2.5. Method for Obtaining UV-Visible Spectra

Time-Dependent Density Functional Theory (TD-DFT) is an extension of Density Functional Theory (DFT) to systems subject to time-dependent perturbations. Based on the Runge-Gross theorem, it establishes that the time-dependent electron density uniquely determines the external potential applied to the system. This approach thus allows for the description of excited electronic states and transitions between different energy levels.

In practice, TD-DFT relies on solving the time-dependent Kohn-Sham equations, in which electrons evolve under the influence of an external perturbation, such as an electromagnetic field. This method is now widely used in quantum chemistry to predict excitation energies, absorption wavelengths, oscillator forces, and the optical properties of molecules and coordination complexes [23].

In this work, the electronic properties of excited states are studied using the TD-B3LYP/LanL2DZ theory, implemented in the Gaussian software package. The calculations allow us to determine the electronic transition energies, absorption wavelengths, oscillator forces, and the nature of the transitions involved. These parameters are then used to simulate and analyze the UV-visible absorption spectra of the ruthenium complexes under study, in order to evaluate the effect of azo ligand substitution on their optical and photochemical properties.

3. Results and Discussion

3.1. Comparison of the Geometry of $RuCl_2L_2$ Complexes

The structures of the compounds studied are derived from those of the γ-$RuCl_2(azpy)_2$ and δ-$RuCl_2(azpy)_2$ isomers by replacing pyridine with pyrimidine or benzene. These compounds differ in the number of nitrogen atoms. Pyridine and pyrimidine contain one and two, respectively. As for benzene, its structure contains no nitrogen atoms. **Figure 2** shows the ground-state structures of the γ-

$RuCl_2L_2$ and δ-$RuCl_2L_2$ isomers (L = azben, azpy, or papm). These structures were obtained following geometric optimization and frequency calculations. Furthermore, these minimum-energy geometries are characterized by the absence of imaginary frequencies. Table 1 summarizes the geometric parameters of the compounds in this minimum-energy state.

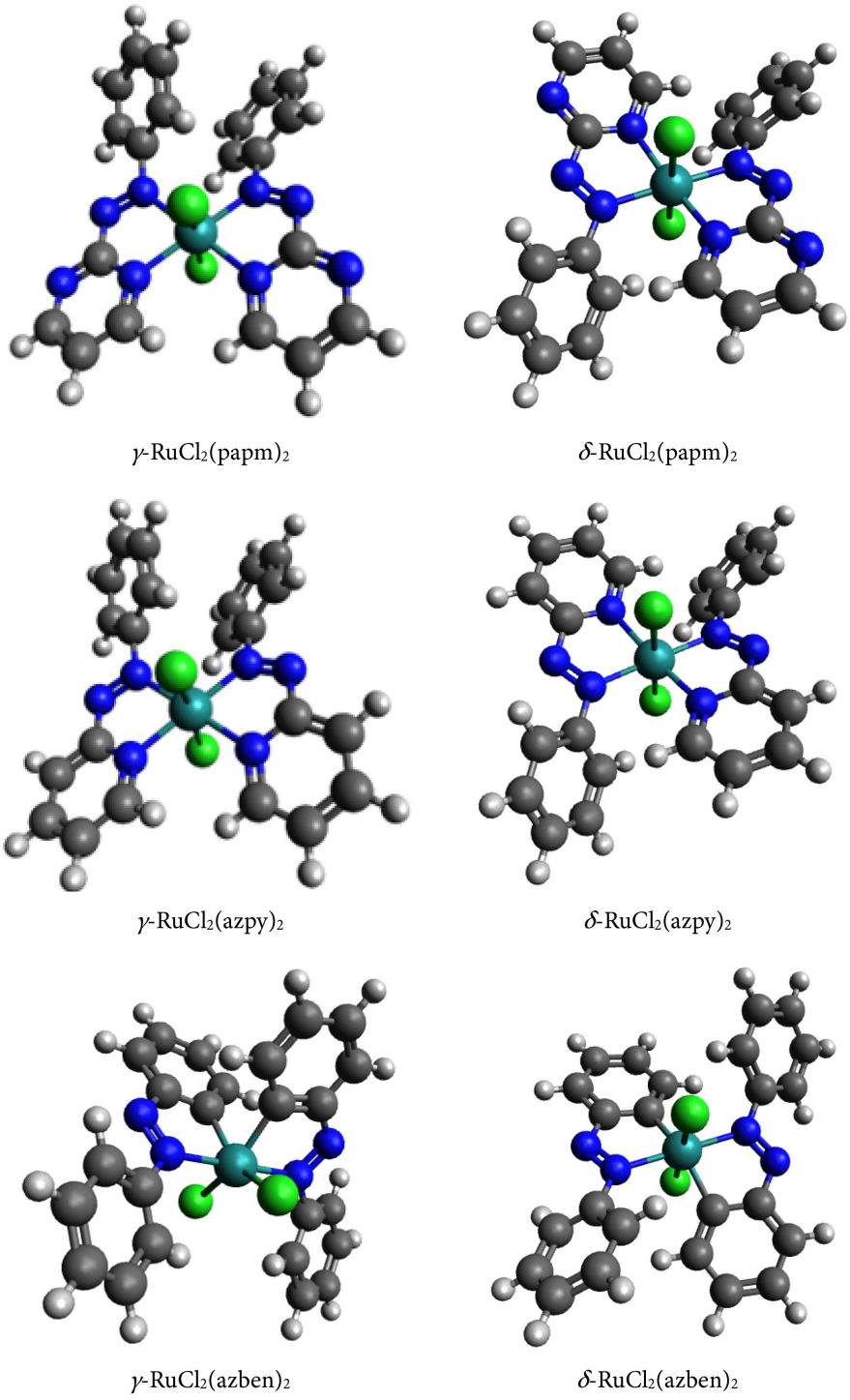

Figure 2. Molecular geometries of the complexes calculated at the B3LYP/Lanl2DZ level.

Table 1. Bond lengths (in Å) and bond angles (in °) involving ruthenium, determined using the B3LYP/Lanl2DZ theory [6] [13].

		$RuCl_2(papm)_2$						
		Ru-Np	Ru-N_2	Ru-Cl	N=N	N_2-Ru-N_2	Np-Ru-Np	Cl-Ru-Cl
***γ*-Cl**	Theo	2.10	2.03	2.47	1.32	105.01	103.56	168.86
	Exp	2.09 2.07	2.00 2.01	2.36 2.40	1.30 1.31	105.53	102.95	169.99
***δ*-Cl**	Theo	2.10	2.06	2.48 2.50	1.31	177.87	166.15	180.00
		$RuCl_2(azpy)_2$						
		Ru-Np	Ru-N_2	Ru-Cl	N=N	N_2-Ru-N_2	Np-Ru-Np	Cl-Ru-Cl
***γ*-Cl**	Théo	2.10	2.03	2.48	1.32	104.95	102.97	170.6
	Exp	2.12 2.10	1.99 1.98	2.38 2.37	1.30 1.31	104.10	103.80	170.5
***δ*-Cl**	Théo	2.10	2.06	2.49 2.51	1.31	177.67	167.43	180.00
	Exp	2.06	2.02	2.38	1.28	180.00	180.00	180.00
		$RuCl_2(azben)_2$						
		Ru-C	Ru-N_2	Ru-Cl	N=N	N_2-Ru-N_2	C-Ru-C	Cl-Ru-Cl
***γ*-Cl**		2.07	2.11	2.42	1.30	179.89	70.33	135.15
***δ*-Cl**		2.05	2.11	2.39 2.58	1.30	179.35	138.82	180.00

Analysis of the geometric data shows that the calculated bond lengths and bond angles are very close to those obtained experimentally. The geometry of the compounds is therefore accurately reproduced by the theoretical calculations. The theoretical approach used is thus suitable for predicting the structure of this type of ruthenium complex. The bond lengths between ruthenium and the two ligand binding sites (N2, Np, or C) range from 2.00 Å to 2.11 Å. In general, the substitution of pyrimidine for pyridine has little effect on the geometry of the ruthenium azopyridine complexes. However, the substitution of pyridine with phenyl, in the case of the *γ*-$RuCl_2(azben)_2$ isomer, profoundly alters the complex's octahedral structure (Np-Ru-Np angle). This difference can be explained, on the one hand, by the Yann-Teller effect and, on the other hand, by repulsive interactions between the free electron pairs on the nitrogen atoms of pyridine and pyrimidine.

3.2. Enthalpy and Spontaneity of the Reaction Leading to the Formation of the Studied Complexes

The spontaneity and enthalpy of a chemical reaction involving the isomers of the

studied complexes are quantified, respectively, by determining the change in reaction enthalpy ($\Delta_r H^\circ$) and the change in reaction free energy ($\Delta_r G^\circ$). A positive value of $\Delta_r H^\circ$ and a positive value of $\Delta_r G^\circ$ indicate, respectively, that the formation reaction under study is endothermic and non-spontaneous at the temperature of study. Conversely, negative changes in these quantities allow these formation reactions to be characterized as exothermic and spontaneous. In addition to these two quantities, the change in entropy ($\Delta_r S^\circ$) accompanying the formation reaction is also considered. A positive value of $\Delta_r S^\circ$ indicates an increase in disorder, whereas a negative value indicates a decrease in disorder. Table 2 presents the values for the change in enthalpy and the change in free enthalpy of the trans isomers of the ruthenium complexes studied.

Table 2. Values of thermodynamic reaction parameters.

Compounds	$\Delta_r H^\circ$ (Kcal/mol)	$\Delta_r S^\circ$ (cal/mol·K)	$\Delta_r G^\circ$ (Kcal/mo)
γ-$RuCl_2(papm)_2$	−13.41	13.28	−17.37
δ-$RuCl_2(papm)_2$	−12.88	15.54	−17.52
γ-$RuCl_2(azpy)_2$	−15.93	9.88	−18.88
δ-$RuCl_2(azpy)_2$	−15.64	13.93	−19.80
γ-$RuCl_2(azben)_2$	802.59	14.54	798.25
δ-$RuCl_2(azben)_2$	807.05	14.92	802.60

The values of the enthalpy changes and free enthalpy for the isomers of the $RuCl_2(papm)_2$ and $RuCl_2(azpy)_2$ complexes are all negative, indicating spontaneous and exothermic formation reactions. In the case of the $RuCl_2(azben)_2$ isomers, the calculated changes are all positive, reflecting non-spontaneous and endothermic reactions at 298 K. Furthermore, examination of the various $\Delta_r G^\circ$ values in Table 2 allows us to establish the following ascending order of reaction spontaneity:

$$\delta\text{-}RuCl_2(azben)_2 < \gamma\text{-}RuCl_2(azben)_2 < \gamma\text{-}RuCl_2(papm)_2 < \delta\text{-}RuCl_2(papm)_2 < \gamma\text{-}RuCl_2(azpy)_2 < \delta\text{-}RuCl_2(azpy)_2$$

This ranking highlights the greater stability of the isomers of ruthenium azopyridine complexes $RuCl_2(azpy)_2$. With regard to the entropy change $\Delta_r S^\circ$, the recorded values range from 9.88 $cal{\cdot}mol^{-1}{\cdot}K^{-1}$ to 15.54 $cal{\cdot}mol^{-1}{\cdot}K^{-1}$. These positive values of $\Delta_r S^\circ$ indicate an increase in disorder during the formation of the compounds studied.

3.3. Comparison of the Overall Reactivity of the Studied Complex Isomers

Frontier molecular orbitals (FMOs) play a key role in the chemical reactivity of compounds. The molecular orbitals of interest are the highest occupied molecular orbital (HOMO) and the lowest unoccupied molecular orbital (LUMO). The dis-

tribution and energies of these various frontier orbitals for the studied compounds are illustrated and compared in Figure 3. Additionally, Table 3 provides information on the percentage contribution of the various atomic entities (ruthenium, chlorine, and ligand) to the formation of the frontier orbitals.

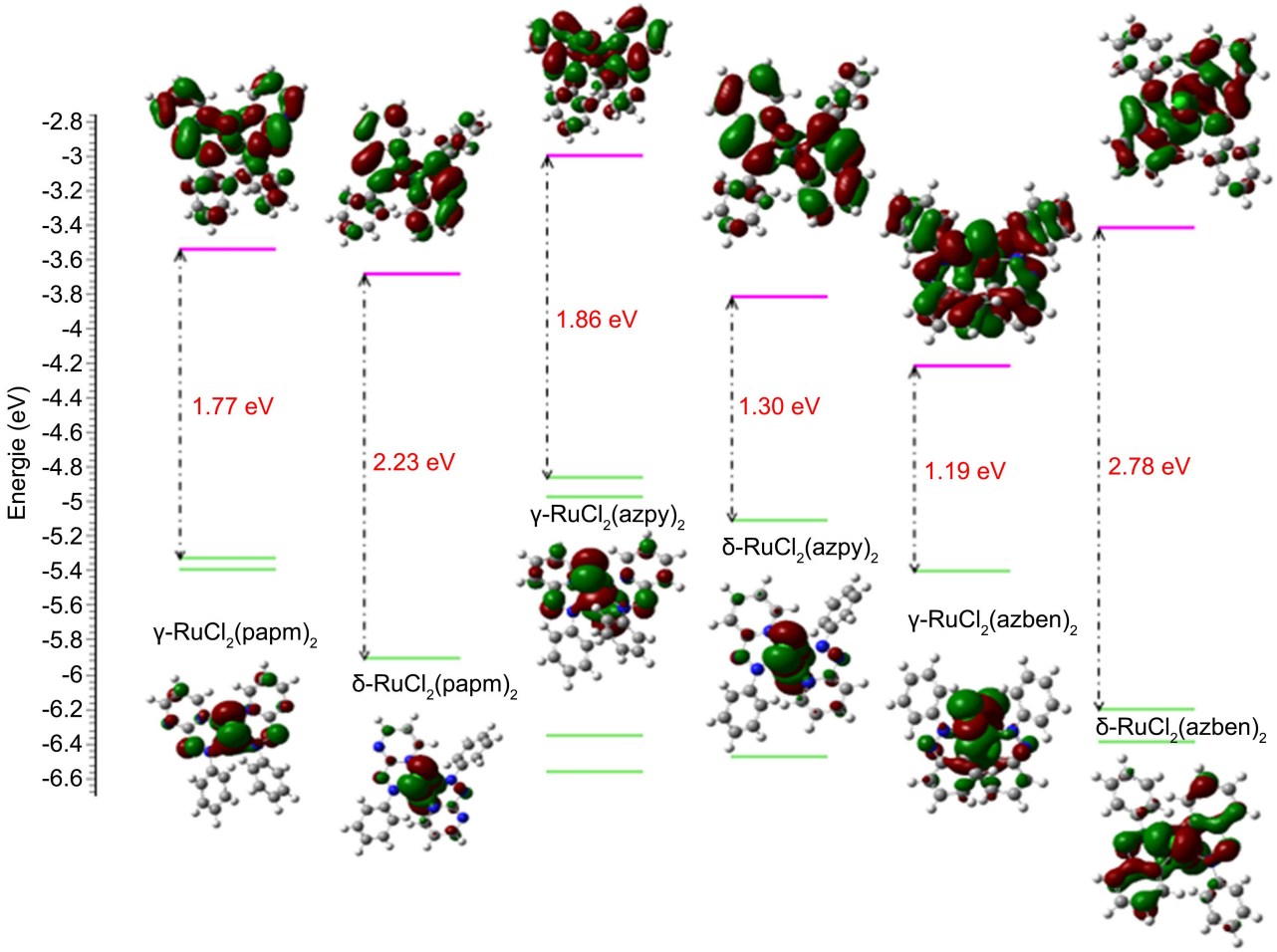

Figure 3. Energy levels and distribution of the frontier orbitals of the compounds studied.

Table 3. Composition of the frontier orbitals of the various complexes.

Compounds	Orbital	Composition in per cent %		
		Ru	Cl	Ligand
γ-$RuCl_2(papm)_2$	HOMO	53	29	17
	LUMO	1	3	96
δ-$RuCl_2(papm)_2$	HOMO	57	31	12
	LUMO	13	2	85
γ-$RuCl_2(azpy)_2$	HOMO	54	28	18
	LUMO	1	3	96

Continued

δ-$RuCl_2(azpy)_2$	HOMO	62	26	12
	LUMO	2	3	95
γ-$RuCl_2(azben)_2$	HOMO	30	30	40
	LUMO	53	22	25
δ-$RuCl_2(azben)_2$	HOMO	46	28	26
	LUMO	27	4	68

Analysis of the distribution of the isodensity surface and the various contributions reveals that ruthenium's contribution to the formation of the compounds' HOMO ranges from 30% to 62%. This significant contribution of ruthenium's d orbitals to the formation of the HOMO shows that the compounds' HOMO is predominantly localized on ruthenium. It is therefore characterized by the ruthenium d orbitals. As for the LUMO of the compounds containing the azpy and papm ligands, it consists of between 1% and 2% of the ruthenium orbitals. The LUMO of these compounds is therefore localized on the ligand. However, the LUMO of the γ and δ isomers of $RuCl_2(azben)_2$ shows contributions from ruthenium's d orbitals of 53% and 27%, respectively. The LUMO of γ-$RuCl_2(azben)_2$ has a metallic character. Thus, for this isomer, ligand-metal transitions (LMCTs) could be observed between its HOMO and LUMO. However, for this compound, MLCT transitions are observed during the electron promotion of the HOMO-1 and HOMO-2 orbitals to the LUMO+1 and LUMO+2 orbitals. The composition of the HOMO and LUMO boundary orbitals of the other compounds favors metal-ligand charge transfer (MLCT) transitions of the $t_{2g} \rightarrow \pi^*$ type.

The energies of these orbitals are listed in the table. They are used to determine the values of the various global reactivity parameters.

Table 4. Global reactivity parameters (in eV).

Composés	HOMO	LUMO	ΔE	μ	η	ω
γ-$RuCl_2(papm)_2$	−5.31	−3.54	1.77	−4.43	0.88	11.15
δ-$RuCl_2(papm)_2$	−5.91	−3.68	2.23	−4.80	1.11	10.38
γ-$RuCl_2(azpy)_2$	−4.86	−3.01	1.86	−3.93	0.93	8.30
δ-$RuCl_2(azpy)_2$	−5.12	−3.82	1.30	−4.47	0.65	15.37
γ-$RuCl_2(azben)_2$	−5.41	−4.22	1.19	−4.82	0.59	19.67
δ-$RuCl_2(azben)_2$	−6.20	−3.42	2.78	−4.81	1.39	8.32

The analysis of the global reactivity descriptors highlights a significant influence of the nature of the ligand and the isomerism on the electronic properties of the studied complexes. Table 4 shows the value of these parameters. In general, a

small HOMO-LUMO energy gap (ΔE) and low chemical hardness (η) are associated with a greater ease of electron-density redistribution and, consequently, enhanced reactivity. Conversely, high values of ΔE and η indicate greater resistance to electronic perturbations and are generally characteristic of more stable systems. Among the studied complexes, γ-$RuCl_2(azben)_2$ appears to be the most reactive, exhibiting the smallest energy gap (ΔE = 1.19 eV) and the lowest chemical hardness (η = 0.59 eV). This high reactivity is further supported by its high electrophilicity index (ω = 19.67 eV), which is the largest value in the series. In contrast, δ-$RuCl_2(azben)_2$ exhibits the largest energy gap (ΔE = 2.78 eV) and the highest chemical hardness (η = 1.39 eV), indicating greater electronic stability and lower reactivity. The other complexes display intermediate behavior. Thus, the substitution of pyridine by benzene in the azben ligand leads to electronic properties that strongly depend on the isomeric form: the γ isomer is characterized by enhanced reactivity, whereas the δ isomer exhibits significantly greater electronic stability. These results suggest that γ-$RuCl_2(azben)_2$ has a particular propensity to participate in interactions involving charge transfer, whereas δ-$RuCl_2(azben)_2$ is distinguished by its greater electronic stability, particularly associated with its high chemical hardness.

By mainly considering ΔE, η, and ω, the following ranking can be proposed:

Increasing reactivity:

$$\delta\text{-}RuCl_2(azben)_2 < \delta\text{-}RuCl_2(papm)_2 < \gamma\text{-}RuCl_2(azpy)_2 < \gamma\text{-}RuCl_2(papm)_2 < \delta\text{-}RuCl_2(azpy)_2 < \gamma\text{-}RuCl_2(azben)_2$$

Conversely, in terms of electronic stability:

$$\gamma\text{-}RuCl_2(azben)_2 < \delta\text{-}RuCl_2(azpy)_2 < \gamma\text{-}RuCl_2(papm)_2 < \gamma\text{-}RuCl_2(azpy)_2 < \delta\text{-}RuCl_2(papm)_2 < \delta\text{-}RuCl_2(azben)_2$$

3.4. Comparison of Electrostatic Potential Distribution

Electrostatic potential maps show the three-dimensional distribution of charges within molecules and allow us to visualize the distribution of charges in a molecule. Understanding this charge distribution helps determine how the molecule interacts with another chemical system. **Figure 4** shows the charge distribution within the various complexes.

A negative electrostatic potential corresponds to an electrophilic site (proton attraction) due to a concentration of electron density (red color on the ESP surface). Conversely, a positive electrostatic potential corresponds to a nucleophilic site (proton repulsion) due to low electron density (shown in blue on the ESP surface). The electrostatic potential increases in the following order of colors: red - orange - yellow - green - blue.

Examination of the surfaces shows that the regions containing the two chlorine atoms and the ruthenium, on the one hand, and the nitrogen atoms not bonded to ruthenium, on the other, are the electrophilic sites. This observation is explained by the presence of free electron pairs on these atoms. The carbon atoms of the various aromatic groups constitute potential nucleophilic attack sites, as indicated by the blue color of these regions.

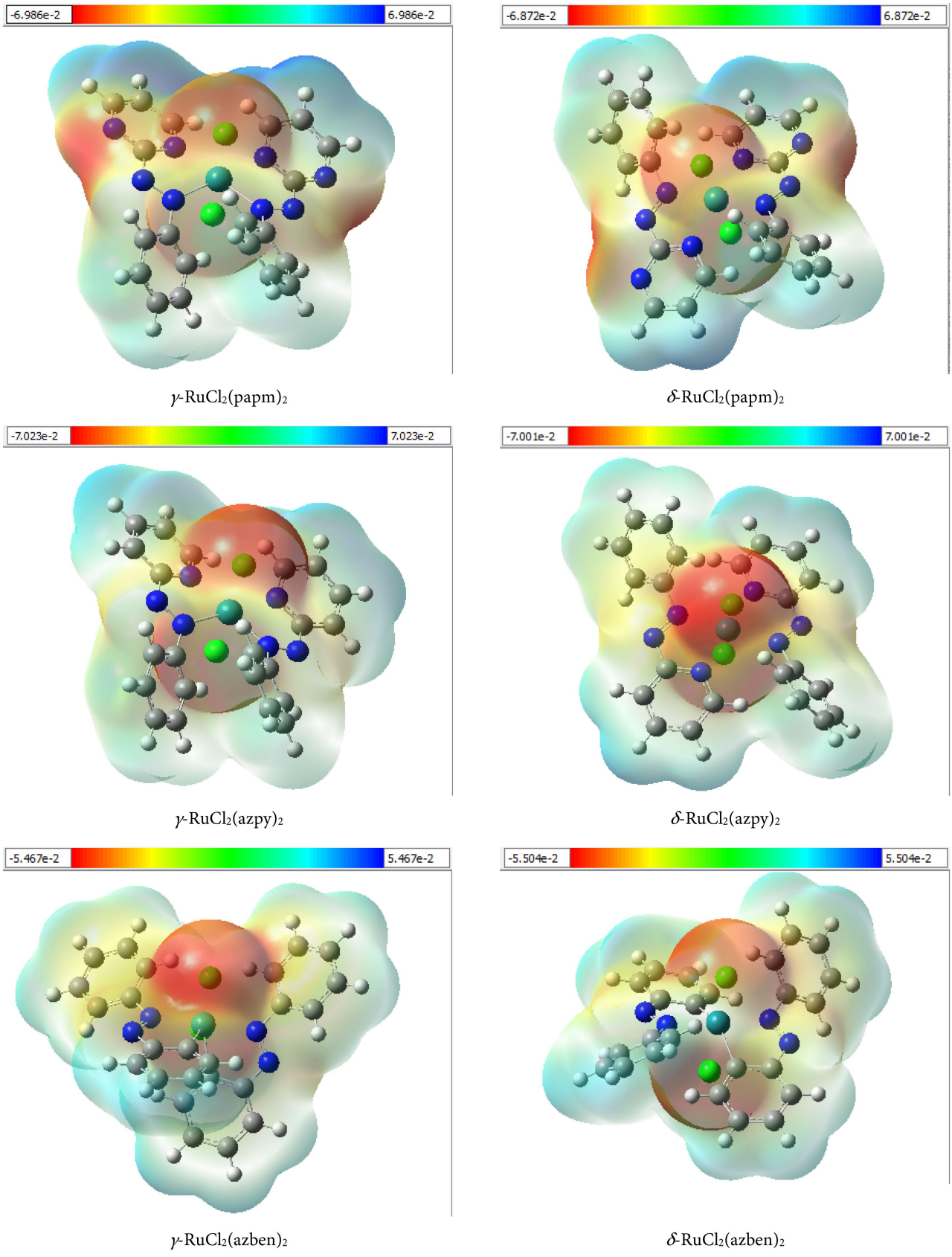

Figure 4. Molecular electrostatic potential surfaces of the complexes studied.

3.5. NBO Analysis of the Structure of the Studied Complexes

The electronic density of the studied complexes is analyzed using the Natural Bond Orbital (NBO) method. The NBO second-order perturbation analysis was carefully reassessed. Only donor-acceptor interactions involving occupied donor orbitals and low-lying unoccupied acceptor orbitals were considered in the discussion. The corresponding stabilization energies were used to identify the main charge-transfer and hyperconjugative interactions contributing to complex stabilization. This provides information on the distribution of electrons among the various atomic orbitals that make up the chemical system. Table 5 illustrates the electronic configuration of the central metal within the studied ruthenium complex isomers. The electron population of ruthenium ranges from 44.00843 to 44.11269 electrons. This deviation from the electron population of the ruthenium atom on its own (44 electrons) is explained by the delocalization of electrons from the nitrogen atoms of the ligand to ruthenium during complex formation. This delocalization is more pronounced in the $RuCl_2(azben)_2$ complexes. These electrons are distributed equally among the core orbitals, valence orbitals, and Rydberg orbitals. In fact, in these compounds, 36 electrons do not participate in the chemical reaction because they occupy the core orbitals, and eight electrons make up the orbitals that may be involved in an interaction or reaction with another chemical system. As for the virtual orbitals, their electron population ranges from 0.03328 to 0.04741. This low population of Rydberg electrons highlights the accuracy and rigor of the theoretical framework used in the distribution of electrons among the various molecular orbitals and, in particular, atomic orbitals. These different orbitals are described using the same atomic orbitals of ruthenium.

Table 5. Electronic configuration of the ruthenium nucleus.

Compounds	Core	Valence	Rydberg	Total	Electronic configuration
γ-$RuCl_2(papm)_2$	35.9823	7.99979	0.04741	44.02959	$[core]5S^{0.28}4d^{7.11}5p^{0.16}5d^{0.03}6p^{0.45}$
δ-$RuCl_2(papm)_2$	35.98322	7.98887	0.0459	44.018	$[core]5S^{0.27}4d^{7.13}5p^{0.20}5d^{0.03}6p^{0.40}$
γ-$RuCl_2(azpy)_2$	35.98233	7.99069	0.04537	44.01839	$[core]5S^{0.28}4d^{7.12}5p^{0.16}5d^{0.03}6p^{0.45}$
δ-$RuCl_2(azpy)_2$	35.98307	7.97927	0.04609	44.00843	$[core]5S^{0.27}4d^{7.12}5p^{0.01}5d^{0.03}6p^{0.59}$
γ-$RuCl_2(azben)_2$	35.96605	8.11369	0.03295	44.11269	$[core]5S^{0.29}4d^{7.16}5p^{0.41}5d^{0.03}6p^{0.26}$
δ-$RuCl_2(azben)_2$	35.95831	8.1055	0.03328	44.09708	$[core]5S^{0.29}4d^{7.21}5p^{0.38}5d^{0.02}6p^{0.24}$

NBO analysis makes it possible to assess the intramolecular interactions that contribute to the stabilization of the molecular structure. This contribution to stability is measured using the second-order perturbation energy E^2. Furthermore, a higher value of the perturbation energy indicates a greater contribution to the stabilization of the compound. Table 6 presents the values of the second-order perturbation energies associated with stabilizing interactions involving ruthenium.

Table 6. Interactions involving ruthenium and associated second-order perturbation energy values in kcal·mol^{-1}.

γ-RuCl$_2$(papm)$_2$			**δ-RuCl$_2$(papm)$_2$**		
Donor	Acceptor	E^2	Donor	Acceptor	E^2
σ(Ru-Cl$_{22}$)	σ*(Ru-Cl$_{23}$)	15.74	LP(2)Cl$_{44}$	LP*(5)Ru	21.29
σ(Ru-Cl$_{23}$)	σ*(Ru-Cl$_{22}$)	15.74	LP(3)Ru	π*(N$_{16}$-N$_{21}$)	13.11
LP(3)Ru	π*(N$_{18}$-N$_{21}$)	12.87	LP(3)Ru	π*(N$_{17}$-N$_{20}$)	13.11
LP(3)Ru	π*(N$_{16}$-N$_{20}$)	12.90	LP(1)N$_{14}$	LP*(4)Ru	66.73
LP(1)N$_{18}$	LP*(4)Ru	99.67	LP(1)N$_{16}$	LP*(4)Ru	94.06
LP(1)N$_{19}$	LP*(4)Ru	78.87	LP(1)N$_{15}$	LP*(4)Ru	66.73
LP(1)N$_{16}$	LP*(4)Ru	99.74	LP(1)N$_{17}$	LP*(4)Ru	94.06
LP(1)N$_{17}$	LP*(4)Ru	78.89	LP(4)Cl	LP*(6)Ru	82.90
γ-RuCl$_2$(azpy)$_2$			**δ-RuCl$_2$(azpy)$_2$**		
Donor	Acceptor	E^2	Donor	Acceptor	E^2
σ(Ru-Cl$_{26}$)	σ*(Ru-Cl$_{27}$)	15.08	LP(3)Ru	π*(N$_{20}$-N$_{25}$)	14.1
σ(Ru-Cl$_{27}$)	σ*(Ru-Cl$_{26}$)	15.08	LP(3)Ru	π*(N$_{21}$-N$_{24}$)	14.1
LP(3)Ru	π*(N$_{22}$-N$_{25}$)	12.81	LP(1)N	LP*(4)Ru	68.62
LP(3)Ru	π*(N$_{20}$-N$_{24}$)	12.81	LP(1)N$_{20}$	LP*(4)Ru	92.75
LP(1)N$_{22}$	LP*(4)Ru	96.82	LP(1)N$_{19}$	LP*(4)Ru	68.62
LP(1)N$_{23}$	LP*(4)Ru	80.13	LP(1)N$_{21}$	LP*(4)Ru	92.75
			LP(2)Cl	LP*(6)Ru	23.61
			LP(4)Cl	LP*(6)Ru	83.11
γ-RuCl$_2$(azben)$_2$			**δ-RuCl$_2$(azben)$_2$**		
Donor	Acceptor	E^2	Donor	Acceptor	E^2
σ(Ru-Cl$_{24}$)	σ*(Ru-C$_{49}$)	12.69	σ(1)Ru-Cl$_{46}$	σ*(1)Ru-Cl$_{47}$	11.09
σ(Ru-Cl)	σ*(1)Ru-C$_{48}$	12.64	σ(1)Ru-Cl$_{47}$	σ*(1)Ru-Cl$_{46}$	23.77
σ(Ru-C$_{48}$)	σ*(1)Ru-Cl$_{25}$	34.89	σ(1)Ru-C$_{48}$	σ*(1)Ru-Cl$_{47}$	15.55
σ(Ru-C$_{49}$)	σ*(1)Ru-Cl$_{24}$	34.83	σ(1)Ru-C$_{49}$	σ*(1)Ru-Cl$_{47}$	15.55
LP(1)N$_{20}$	LP*(3)Ru	71.55	LP(1)N$_{18}$	LP*(3)Ru	72.04
LP(1)N$_{20}$	LP*(4)Ru	40.94	LP(1)N$_{18}$	LP*(4)Ru	33.35
LP(1)N$_{20}$	σ*(1)Ru-C$_{48}$	12.41	LP(1)N$_{18}$	σ*(1)Ru-C$_{48}$	11.23
LP(1)N$_{21}$	LP*(3)Ru	71.55	LP(1)N$_{18}$	σ*(1)Ru-C$_{49}$	12.78
LP(1)N$_{21}$	LP*(4)Ru	40.94	LP(1)N$_{19}$	LP*(3)Ru	72.04
LP(1)N$_{21}$	σ*(1)Ru-C$_{49}$	12.41	LP(1)N$_{19}$	LP*(4)Ru	33.35
LP(3)Cl	LP*(5)Ru	16.26	LP(1)N$_{19}$	σ*(1)Ru-C$_{48}$	12.78
LP(3)Cl$_{25}$	LP*(5)Ru	16.26	LP(1)N$_{19}$	σ*(1)Ru-C$_{49}$	11.23

An examination of the E^2 energy values for the $RuCl_2(papm)_2$ isomers indicates that the interactions between the lone pair LP(1)N and the antibonding LP*(4) Ru orbital are associated with the highest second-order perturbation energy values (99.74 kcal·mol^{-1}, 99.67 kcal·mol^{-1}, and 94.06 kcal·mol^{-1}). The recorded E^2 values show that, regardless of the ligand, the interactions between the ligand's bonds or free doublets and the ruthenium orbitals have higher energy. They reflect electron donation from the ligand (papm, azpy, or azben) to ruthenium. Indeed, within the complexes, the delocalization of the π electrons from the azo group has the effect of stabilizing the complex. This greater energy transfer is indicative of a ligand-metal transition (LMCT) at low wavelengths. However, stabilizing interactions between the ruthenium d orbitals and the π*(N=N) orbitals of the azo bond or the free doublets of the chlorine atoms are observed. These interactions result in electron back-donation. The papm, azpy, and azben ligands are therefore electron acceptors. This delocalization of ruthenium's electron density—which is less significant—stabilizes the resulting complex. This type of interaction is responsible for electron transfers from ruthenium to the ligand (MLTC), which can be exploited in photodynamic therapy.

3.6. Effect of Substitution on Spectroscopic Properties

Azo compounds are known for their photochromic properties. The spectroscopic properties of these compounds were studied in vacuum and in acetonitrile using time-dependent DFT at the TD-B3LYP/Lanl2DZ level. Figure 5 compares the absorption spectra obtained in the solvent.

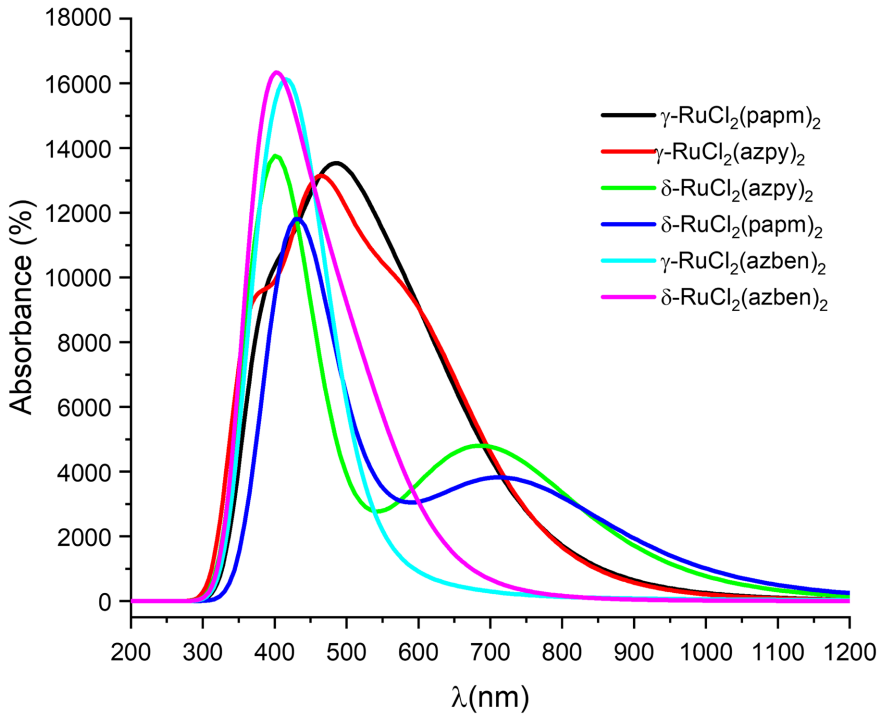

Figure 5. UV-visible spectra in acetonitrile of the various complexes studied.

Table 7. Characteristic parameters (excitation energy E_{exc}, wavelength λ, and oscillator strength f) of the UV-visible spectra of the complexes studied [6].

	E_{exc} (eV)	λ (nm)	f		E_{exc} (eV)	λ (nm)	f
	γ-$RuCl_2(papm)_2$				δ-$RuCl_2(papm)_2$		
Vacuum	2.05	604.24	0.09	**Vacuum**	1.46	848.63	0.05
	2.58	480.30	0.12		3.04	407.38	0.11
Acetonitrile	1.76	705.18	0.02	**Acetonitrile**	1.69	734.50	0.09
	2.10	589.67	0.16		2.76	448.52	0.15
	2.55	485.99	0.21				
Acetonitrile (Exp.)		723					
		528					
		433					
	γ-$RuCl_2(azpy)_2$				δ-$RuCl_2(azpy)_2$		
Vacuum	2.04	606.40	0.10	**Vacuum**	1.50	825.90	0.06
	2.64	469.62	0.12		3.14	394.41	0.16
Acetonitrile	2.11	587.13	0.18	**Acetonitrile**	1.77	700.51	0.11
	2.67	463.63	0.23		2.93	423.70	0.17
	γ-$RuCl_2(azben)_2$				δ-$RuCl_2(azben)_2$		
Vacuum	2.70	458.29	0.01	**Vacuum**	2.63	470.96	0.06
	2.84	436.90	0.09		3.24	382.21	0.11
Acetonitrile	2.75	450.00	0.09	**Acetonitrile**	2.39	519.23	0.08
	3.20	386.86	0.08		3.2	377.91	0.18

The wavelength values obtained experimentally and those obtained by calculation are very close (as shown in Table 7). The B3LYP functional and the Lanl2DZ pseudopotential used are therefore appropriate for simulating and predicting the UV-visible absorption spectra of ruthenium complexes. The interaction of these compounds with light gives rise to two types of electronic transitions. The first type of transition, observed at wavelengths below 400 nm, consists of intra-ligand transitions (LLCTs). The transitions observed between 400 nm and 800 nm are metal-ligand transitions (MLCTs). This latter type of transition is responsible for the photochemical properties of ruthenium complexes.

The spectra of the δ-$RuCl_2(papm)_2$ and δ-$RuCl_2(azpy)_2$ isomers exhibit a very intense band centered at 400 nm and a second, much weaker band centered at 700 nm. The transitions associated with these bands are of the intra-ligand LLCT and metal-ligand MLCT types, respectively. The substitution of pyrimidine for pyridine results in a slight bathochromic effect (shift toward longer wavelengths) ac-

companied by a more or less significant hypochromic effect (decrease in absorption intensity). In the case of the isomers γ-$RuCl_2(papm)_2$ and γ-$RuCl_2(azpy)_2$, the absorption spectra have the same profile and exhibit a single intense band centered at 589.674 nm and 463.634 nm, respectively. These bands reveal MLCT transitions with an absorption intensity greater than that of the δ-$RuCl_2L_2$ isomers. Additionally, shoulders are observed on either side of the intense band. The left shoulder, located at a wavelength below 400 nm, is characteristic of an intra-ligand transition. Furthermore, the substitution of pyrimidine for pyridine also produces a slight bathochromic and hypsochromic effect. However, the substitution of pyridine with benzene affects the shape of the complex's absorption spectrum, which now exhibits only a single intense absorption band centered at 382.209 nm for δ-$RuCl_2(azben)_2$ and at 436.905 nm for γ-$RuCl_2(azben)_2$. These bands are characteristic of intra-ligand transitions. Furthermore, metal-ligand transitions in these compounds, observed at 450.003 nm for γ-$RuCl_2(azben)_2$ and at 519.230 nm for δ-$RuCl_2(azben)_2$, show that cyclomethylation has a significant hypsochromic effect (shifts toward shorter wavelengths) on this transition. Overall, the results reveal a structure-property relationship in which the nature of the aromatic ring and the geometric arrangement of the ligands around ruthenium significantly modulate the absorption properties. The MLCT transitions located in the visible range especially pronounced for certain γ isomers give these complexes potential interest for photophysical and photochemical applications.

4. Conclusions

The objective of this work was to evaluate the influence of the nature of the azo ligand's aromatic ring on the geometric, thermodynamic, electronic, and spectroscopic properties of ruthenium complexes of the general formula $RuCl_2L_2$ (L = papm, azpy, or azben), using density functional theory (DFT) and its time-dependent extension (TD-DFT) at the B3LYP/LanL2DZ theory level.

The results show that replacing the ligand's aromatic ring has little effect on the coordination geometry around the metal center. The characteristic bond lengths and angles of ruthenium remain largely unchanged, reflecting the robustness of the octahedral environment of the complexes studied.

The thermodynamic study reveals that the reactions leading to the formation of isomers of the $RuCl_2(papm)_2$ and $RuCl_2(azpy)_2$ complexes are spontaneous and exothermic at 298.15 K, unlike those of the $RuCl_2(azben)_2$ complexes, which become favorable only at higher temperatures. The azopyridine-derived complexes thus appear to be the most thermodynamically stable.

Analysis of frontier orbitals and global reactivity descriptors reveals a significant influence of the ligand's nature on the electronic properties. Replacing azopyridine with azobenzene increases the complexes' electronic reactivity and enhances their ability to transfer charge. Among the compounds studied, the γ-$RuCl_2(azben)_2$ isomer exhibits the electronic characteristics most conducive to interactions with DNA bases, suggesting interesting biological potential.

The spectroscopic study conducted using TD-DFT shows that all of the complexes absorb in the visible region. The observed electronic transitions are primarily of the Metal-to-Ligand Charge Transfer (MLCT) type, characteristic of ruthenium complexes. These optical properties confirm their potential utility as photosensitizers in dynamic phototherapy applications for cancer treatment.

Overall, this study highlights that modifying the nature of the ligand's aromatic ring is a relevant strategy for modulating the electronic properties, reactivity, and optical properties of ruthenium complexes. The results thus provide useful insights for the rational design of new organometallic complexes intended for biomedical and photochemical applications.

Looking ahead, it would be interesting to:

- study the interactions of these complexes with biomolecules of therapeutic interest (DNA, target proteins, or enzymes) using molecular docking and molecular dynamics approaches to better understand their mechanisms of action;
- to examine the effect of increasing the number of nitrogen atoms or extending the conjugation of the ligands on the electronic, spectroscopic, and biological properties of the complexes;
- to explicitly evaluate the photophysical properties (fluorescence yield, excited-state lifetimes, singlet oxygen production) in order to assess their potential in dynamic phototherapy;
- finally, to compare theoretical predictions with experimental results from synthesis, characterization, and biological evaluation in order to validate the trends revealed by quantum calculations.

Author Contributions

N'Guessan Kouakou Nobel: Initiating Author; Kangah Niamké Jean Baptiste: Initiating Author; Koné Mamadou Guy-Richard: Initiating Author.

Conflicts of Interest

The authors declare no conflicts of interest regarding the publication of this paper.

References

[1] De Filippis, B., Della Valle, A., Ammazzalorso, A., Maccallini, C., Tesse, G., Amoroso, R., *et al.* (2024) Azobenzene as Multi-Targeted Scaffold in Medicinal Chemistry. *Molecules*, **29**, Article 5872. https://doi.org/10.3390/molecules29245872

[2] Aykut, D., Alpaslan, B., Hazal, K., Pinar, T.T. and Fati, Y. (2023) Obtaining of Novel Pyrazolo Pyrimidine Disazo Dyes Derived from 4-Position and a Theoretical and Experimental Comparison of Their Characteristic Properties. Research Square. https://doi.org/10.21203/rs.3.rs-2521954/v1

[3] Dembitsky, V.M. and Terent'ev, A.O. (2025) Azo Dyes and the Microbial World: Synthesis, Breakdown, and Bioactivity. *Microbiology Research*, **16**, Article 100. https://doi.org/10.3390/microbiolres16050100

[4] Affi, S.T., Bamba, K. and Ziao, N. (2015) Computational Characterization of Organometallic Ligands Coordinating Metal: Case of Azopyridine Ligands. *Journal of The-*

oretical and Computational Chemistry, **14**, Article ID: 1550006. https://doi.org/10.1142/s0219633615500066

[5] Mohamed, M.S., Awad, S.M., El-tawab, N.A.A. and Ahmed, N.M. (2022) An Overview on Synthesis and Biological Activity of Pyrimidines. *World Journal of Advanced Research and Reviews*, **15**, 272-296. https://doi.org/10.30574/wjarr.2022.15.1.0689

[6] Santra, P.K., Misra, T.K., Das, D., Sinha, C., Slawin, A.M.Z. and Woollins, J.D. (1999) Chemistry of Azopyrimidines. Part II. Synthesis, Spectra, Electrochemistry and X-Ray Crystal Structures of Isomeric Dichloro Bis[2-(Arylazo)Pyrimidine] Complexes of Ruthenium(II). *Polyhedron*, **18**, 2869-2878. https://doi.org/10.1016/s0277-5387(99)00189-8

[7] Hotze, A.C.G., Caspers, S.E., de Vos, D., Kooijman, H., Spek, A.L., Flamigni, A., *et al.* (2004) Structure-Dependent *in Vitro* Cytotoxicity of the Isomeric Complexes $[Ru(L)_2Cl_2]$ (L = *o*-Tolylazopyridine and 4-Methyl-2-Phenylazopyridine) in Comparison to $[Ru(azpy)_2Cl_2]$. *JBIC Journal of Biological Inorganic Chemistry*, **9**, 354-364. https://doi.org/10.1007/s00775-004-0531-6

[8] Misra, T.K., Das, D., Sinha, C., Ghosh, and Pal, C.K. (1998) Chemistry of Azoimidazoles: Synthesis, Spectral Characterization, Electrochemical Studies, and X-Ray Crystal Structures of Isomeric Dichloro Bis[1-Alkyl-2-(Arylazo)Imidazole] Complexes of Ruthenium(II). *Inorganic Chemistry*, **37**, 1672-1678. https://doi.org/10.1021/ic970446p

[9] Nobel, N.K., Kangah, N.J.B., Missa, E.J., Stéphane, D.G., Patrice, O.W., Bamba, K., *et al.* (2025) Structure-Activity Relationships of Substituted Ruthenium Azopyridine Complexes: A DFT and QSAR Study for Anticancer Applications. *Chemical Science International Journal*, **34**, 70-85. https://doi.org/10.9734/csji/2025/v34i2958

[10] N'guessan, K.N., Guy-Richard Koné, M., Bamba, K., Wawohinlin Patrice, O. and Ziao, N. (2017) Quantitative Structure Anti-Cancer Activity Relationship (QSAR) of a Series of Ruthenium Complex Azopyridine by the Density Functional Theory (DFT) Method. *Computational Molecular Bioscience*, **7**, 19-31. https://doi.org/10.4236/cmb.2017.72002

[11] Hotze, A.C.G., van der Geer, E.P.L., Caspers, S.E., Kooijman, H., Spek, A.L., Haasnoot, J.G., *et al.* (2004) Coordination of 9-Ethylguanine to the Mixed-Ligand Compound *α*-$[Ru(azpy)(bpy)Cl_2]$ (azpy = 2-Phenylazopyridine and bpy = 2,2'-Bipyridine). An Unprecedented Ligand Positional Shift, Correlated to the Cytotoxicity of This Type of $[RuL_2Cl_2]$ (with L = azpy or bpy) Complex. *Inorganic Chemistry*, **43**, 4935-4943. https://doi.org/10.1021/ic035390f

[12] Krause, R.A. and Krause, K. (1980) Chemistry of Bipyridyl-Like Ligands. Isomeric Complexes of Ruthenium(II) with 2-(Phenylazo)Pyridine. *Inorganic Chemistry*, **19**, 2600-2603. https://doi.org/10.1021/ic50211a024

[13] Velders, A.H., van der Schilden, K., Hotze, A.C.G., Reedijk, J., Kooijman, H. and Spek, A.L. (2004) Dichlorobis(2-Phenylazopyridine)Ruthenium(II) Complexes: Characterisation, Spectroscopic and Structural Properties of Four Isomers. *Dalton Transactions*, No. 3, 448-455. https://doi.org/10.1039/b313182c

[14] Nobel, N.K., Bamba, K., Patrice, O.W. and Ziao, N. (2017) Theoretical Investigation of the Structure Activity Relationships (SARs) of a Series of Five Isomeric *α*, *β*, *γ*, *δ*, *ε* Ruthenium Complexes $RuCl_2L_2$ with Azopyridine Ligands [L= azpy, tazpy, 4mazpy, 5mazpy]. *International Journal of Engineering Research and Applications*, **7**, 58-70. https://doi.org/10.9790/9622-0706015870

[15] Lu, L., Hu, H., Hou, H. and Wang, B. (2013) An Improved B3LYP Method in the Calculation of Organic Thermochemistry and Reactivity. *Computational and Theo-*

retical Chemistry, **1015**, 64-71. https://doi.org/10.1016/j.comptc.2013.04.009

[16] Chiodo, S., Russo, N. and Sicilia, E. (2006) LANL2DZ Basis Sets Recontracted in the Framework of Density Functional Theory. *The Journal of Chemical Physics*, **125**, Article ID: 104107. https://doi.org/10.1063/1.2345197

[17] Frisch, M.J., Trucks, G.W., Schlegel, H.B., Scuseria, G.E., Robb, M.A., Cheeseman, J.R., *et al.* (2009) Gaussian 09, Revison A.02. Wallingford Center Inc.

[18] Kone, M.G., Ouattara, L., N'Guessan, K.N., Dembele, G.S., Karamanis, P. and Ziao, N. (2024) Theoretical Study of the Stability and Chemical Reactivity of a Series of Dihydropyrazoles with Antiproliferative Activities. *Chemical Science International Journal*, **33**, 102-113. https://doi.org/10.9734/csji/2024/v33i6929

[19] Kan Lucien Yao, N., Soro, D., Nobel N'Guessan, K., Benié, A., Dembele, S., Akoua Kouassi-Yao, P., *et al.* (2025) A Comparative DFT Study of the Chemical Reactivity of Diastereoisomers Cis/Trans Clovamides and Derivatives, Isolated from *Icacina mannii*. *Journal of Materials Physics and Chemistry*, **13**, 8-15. https://doi.org/10.12691/jmpc-13-1-2

[20] Ritter, S. (2003) Hard and Soft Acids and Bases. *Chemical & Engineering News Archive*, **81**, 50. https://doi.org/10.1021/cen-v081n007.p050

[21] Melnikov, F., Geohagen, B.C., Gavin, T., LoPachin, R.M., Anastas, P.T., Coish, P., *et al.* (2020) Application of the Hard and Soft, Acids and Bases (HSAB) Theory as a Method to Predict Cumulative Neurotoxicity. *NeuroToxicology*, **79**, 95-103. https://doi.org/10.1016/j.neuro.2020.04.009

[22] Ulaş, Y. (2020) Natural Bond Orbital (NBO) Population Analysis and Non-Linear Optical (NLO) Properties of 2-(Azepan-1-yl(Naphthalen-1-yl)Methyl)Phenol. *International Journal of Chemistry and Technology*, **4**, 138-145. https://doi.org/10.32571/ijct.751001

[23] N'guessan, N.K., Bamba, K., Patrice, O.W. and Ziao, N. (2018) Theoretical Investigation of Structural and Electronic Properties of Ruthenium Azopyridine Complexes Dyes for Photovoltaic Applications by Using DFT and TD-DFT Methods. *European Scientific Journal, ESJ*, **14**, 424. https://doi.org/10.19044/esj.2018.v14n21p424